

Reduced Graphene Oxide/Copper Nanowire Hybrid Films as High-Performance Transparent Electrodes

Iskandar N. Kholmanov, Sergio H Domingues, Harry Chou, Xiaohan Wang, Cheng Tan, Jin-Young Kim, Huifeng Li, Richard Piner, Aldo JG Zarbin, and Rodney S. Ruoff

ACS Nano, **Just Accepted Manuscript** • DOI: 10.1021/nn3060175 • Publication Date (Web): 29 Jan 2013

Downloaded from <http://pubs.acs.org> on February 5, 2013

Just Accepted

“Just Accepted” manuscripts have been peer-reviewed and accepted for publication. They are posted online prior to technical editing, formatting for publication and author proofing. The American Chemical Society provides “Just Accepted” as a free service to the research community to expedite the dissemination of scientific material as soon as possible after acceptance. “Just Accepted” manuscripts appear in full in PDF format accompanied by an HTML abstract. “Just Accepted” manuscripts have been fully peer reviewed, but should not be considered the official version of record. They are accessible to all readers and citable by the Digital Object Identifier (DOI®). “Just Accepted” is an optional service offered to authors. Therefore, the “Just Accepted” Web site may not include all articles that will be published in the journal. After a manuscript is technically edited and formatted, it will be removed from the “Just Accepted” Web site and published as an ASAP article. Note that technical editing may introduce minor changes to the manuscript text and/or graphics which could affect content, and all legal disclaimers and ethical guidelines that apply to the journal pertain. ACS cannot be held responsible for errors or consequences arising from the use of information contained in these “Just Accepted” manuscripts.



1
2
3
4
5
6
7
8
9
10
11
12
13
14
15
16
17
18
19
20
21
22
23
24
25
26
27
28
29
30
31
32
33

Reduced Graphene Oxide/Copper Nanowire Hybrid Films as High-Performance Transparent Electrodes

Iskandar N. Kholmanov^{†,§}, Sergio H. Domingues^{†,¶}, Harry Chou[†], Xiaohan Wang[†], Cheng Tan[†],
JinYoung Kim[†], Huifeng Li[†], Richard Piner[†], Aldo J. G. Zarbin[¶], Rodney S. Ruoff^{†*}

[†]Department of Mechanical Engineering and the Materials Science and Engineering Program,
The University of Texas at Austin, 1 University Station C2200, Austin, TX 78712, USA

[‡]CNR-IDASC Sensor Lab Department of Chemistry and Physics, University of Brescia, via
Valotti, 9, Brescia 25133, Italy,

[¶]Department of Chemistry, Universidade Federal do Paraná, CP 19081, CEP 81531-990,
Curitiba, PR, Brazil.

34
35
36
37
38
39
40
41
42
43
44
45
46
47
48
49
50
51
52
53
54
55
56
57
58
59
60

Abstract. Hybrid films composed of reduced graphene oxide (RG-O) and Cu nanowires (NWs) were prepared. Compared to Cu NW films, the RG-O/Cu NW hybrid films have improved electrical conductivity, oxidation-resistance, substrate adhesion, and stability in harsh environments. The RG-O/Cu NW films were used as transparent electrodes in Prussian blue (PB)-based electrochromic devices where they performed significantly better than pure Cu NW films.

Keywords: reduced graphene oxide, copper nanowires, hybrid films, transparent conductive films.

The electrical and optical properties of metal nanowire (NW) films make them promising materials for transparent conductive film (TCF) applications. It has been demonstrated that Au NW,^{1,2} Ag NW^{3,4} and Cu NW films⁵⁻⁷ can have sheet resistances (R_s) comparable to or lower than commonly used indium tin oxide (ITO) films at the same optical transmittance (T). Metal

1
2
3 NW films on plastic substrates can have better mechanical properties than ITO films for flexible
4 electronics.⁴⁻⁶ However, metal NW films can have low oxidation-resistance, poor adhesion to the
5 substrate, and low stability in harsh environments. NW films have electrically non-conductive
6 open spaces while some applications require continuously conductive regions. One strategy to
7 overcome the drawbacks of metal NW films involves the addition of components such as metal
8 nanoparticles, thin metal films, oxide nanostructures, or conductive polymers.⁸⁻¹² Typically the
9 added constituent can only address one of the weaknesses of NW films and adding multiple
10 constituents may lead to processing and cost-related issues.

11
12 In this context, reduced graphene oxide (RG-O) offers versatile functional properties.¹³⁻¹⁷
13 We recently demonstrated¹⁸ that the addition of RG-O into metal NW films resulted in hybrid
14 films with improved electrical conductivity, as RG-O provides two-dimensional pathways for
15 charge transfer between non-percolated metal NWs. Here, we show that RG-O platelets
16 deposited on top of Cu NW films simultaneously address multiple problems, acting as an
17 oxidation-resistive layer; a conductive and continuous transparent film that fills in open spaces
18 between NWs; and an additional material that protects the NWs from harsh environments.

19 20 21 22 23 24 25 26 27 28 29 30 31 32 33 34 35 36 37 38 39 40 41 **RESULTS AND DISCUSSION**

42
43 Cu NWs (average length >20 μm , average diameter <60 nm, purchased from Nanoforge)
44 were dispersed in a mixture of 97.0 vol% isopropyl alcohol (IPA) and 3.0 vol% hydrazine
45 monohydrate ($\text{N}_2\text{H}_4 \cdot \text{H}_2\text{O}$), at a concentration of ~ 1.2 mg/mL. Spray coating of this dispersion
46 onto a target substrate yields a thin film of randomly oriented Cu NWs with open spaces between
47 them (Figure 1a). RG-O films were fabricated by spin coating a dispersion of graphene oxide (G-
48 O) platelets, followed by chemical and thermal reduction processes (see Methods). The resulting
49
50
51
52
53
54
55
56
57
58
59
60

1
2
3 RG-O films have a continuous and smooth surface morphology, as shown by atomic force
4
5
6 microscopy (AFM) in Figure 1b.

7
8 The sheet resistance and optical transmittance of the Cu NW and RG-O films are listed in
9
10 Figure 1c. To improve electrical conductivity the as-deposited Cu NW films were annealed in a
11
12 tube furnace at 180 °C for 30 min under Ar (95%) +H₂ (5 %) at 1 atm pressure. The Cu NW
13
14 films with an optical transmittance at 550 nm of $T_{550} > 95\%$ had no globally connected network
15
16 of NWs (*i.e.* the films were non-conductive). Longer spraying time increases the density of NWs,
17
18 yielding percolated networks, and decreases both the T_{550} and R_s of the films. Typical films with
19
20 $T_{550} = 90\%$ have a sheet resistance of $R_s = 295 \pm 19.5 \Omega/\text{sq}$. Typical RG-O films with $T_{550} = 90\%$
21
22 have a sheet resistance of $R_s = 19.6 \pm 2.7 \text{ k}\Omega/\text{sq}$. Contributing to the R_s of the RG-O films are
23
24 structural defects and junction resistances between RG-O platelets.¹⁸

25
26
27
28
29 Figure 2a shows a schematic detailing the assembly process of RG-O films onto Cu NW
30
31 films. The dispersions of the Cu NWs (1.2 mg/mL) and G-O (1.0 mg/mL) shown in Figure 2b
32
33 were used to produce thin films (Figure 2c) of Cu NWs and RG-O by spray and spin coating,
34
35 respectively. A poly(methyl methacrylate) (PMMA) was spin coated on top of the RG-O films,
36
37 and the resulting PMMA/RG-O film was subsequently delaminated from the glass substrate in
38
39 1M NaOH aqueous solution (Figure 2d), as described elsewhere.¹⁹ The delaminated PMMA/RG-
40
41 O films were washed several times with de-ionized (DI) water in order to remove the residual
42
43 NaOH, and then transferred on top of Cu NW films using a dry transfer method.^{20, 21} After
44
45 transfer, the PMMA layer was removed with acetone, resulting in the final RG-O/Cu NW hybrid
46
47 films as shown in Figure 2e. To improve electrical conductivity, the obtained RG-O/Cu NW
48
49 films were annealed in a tube furnace at 180 °C for 30 min under a Ar (95%) +H₂ (5 %) gas
50
51 mixture at 1 atm pressure.
52
53
54
55
56
57
58
59
60

1
2
3
4
5
6
7
8
9
10
11
12
13
14
15
16
17
18
19
20
21
22
23
24
25
26
27
28
29
30
31
32
33
34
35
36
37
38
39
40
41
42
43
44
45
46
47
48
49
50
51
52
53
54
55
56
57
58
59
60

Figure 3a shows sheet resistances and optical transmittances of the composite films. The RG-O films used in the hybrid film fabrication had $R_s = 36.6 \pm 4.7 \text{ k}\Omega/\text{sq}$ and $T_{550} = 95.5 \%$. The hybrid films had $R_s = 34 \pm 2.6 \text{ }\Omega/\text{sq}$ at $T_{550} = 80\%$, which can be compared to pure Cu NW films ($R_s = 51 \pm 4.0 \text{ }\Omega/\text{sq}$) and pure RG-O films ($R_s = 7.6 \pm 0.86 \text{ k}\Omega/\text{sq}$), each also at $T_{550} = 80\%$. Individual Cu NWs with an average length $>20 \text{ }\mu\text{m}$ can connect two or more RG-O platelets, and the metallic conductivity of these NWs can decrease or eliminate the platelet-platelet junction resistance.¹⁸ In turn, the film of overlapped and stacked RG-O platelets can bridge initially non-connected Cu NWs. The lateral size of RG-O platelets may be as large as several micrometers, as shown in Figure 3b. A single RG-O platelet with such a lateral size can bridge two or more non-connected Cu NWs separated by any distance smaller than the lateral size of the platelet. This may results in higher electrical conductivity of the hybrid films because of the absence of RG-O inter-platelet junction resistances. Without RG-O platelets, the non-connected Cu NWs cannot contribute to the electrical conductivity of the Cu NW films. The continuous RG-O film also eliminates the empty spaces between NWs, as shown in Figure 3c, and provides a two dimensional conductive platform for charge carriers, which is particularly attractive for dye-sensitized solar cells.²² Overall, the synergy between Cu NWs and RG-O platelets allow for the fabrication of the hybrid films with electrical conductivity better than pure RG-O and pure Cu NW films.

The RG-O film can also protect the Cu NWs underneath it from oxidation resulting in improved stability of the hybrid film. Figure 4a shows the change of R_s over time of pure Cu NW and hybrid RG-O/Cu NW films in ambient atmosphere at room temperature and at $60 \text{ }^\circ\text{C}$. The room temperature R_s of Cu NW films increases from $57 \pm 2.5 \text{ }\Omega/\text{sq}$ (as-prepared sample) to $69 \pm 3.2 \text{ }\Omega/\text{sq}$ after 72 hours, and the R_s of the samples at $60 \text{ }^\circ\text{C}$ increases from $56 \pm 2.5 \text{ }\Omega/\text{sq}$ (as-

1
2
3 prepared sample) to $94 \pm 4.7 \text{ } \Omega/\text{sq}$ also after 72 hours. The change in R_s values is due to the
4
5 oxidation of the Cu NW films, and the more rapid increase at $60 \text{ } ^\circ\text{C}$ is due to the faster kinetics
6
7 of oxidation at higher temperatures.¹⁰ The R_s of the hybrid RG-O/Cu NW films show no
8
9 significant change after 72 hours at room temperature and also at $60 \text{ } ^\circ\text{C}$. This is consistent with
10
11 Raman spectroscopy studies (Figure 4b). Cu NW films, kept at room temperature for 72 hours,
12
13 show Raman peaks at about 214, 460, and 644 cm^{-1} . The Raman spectrum of the Cu NW films
14
15 kept at $60 \text{ } ^\circ\text{C}$ for 72 hours exhibit the same peaks but with higher intensity, and several
16
17 additional peaks in the range of $200 - 800 \text{ cm}^{-1}$. These Raman peaks are due to different copper
18
19 oxides: CuO (299, 342, 500, 634 cm^{-1}), Cu₂O (214, 644 cm^{-1}), Cu(OH)₂ ($450 - 470 \text{ cm}^{-1}$, $540 -$
20
21 580 cm^{-1}).²³⁻²⁵ The higher intensity Raman peaks of the Cu NW films held at $60 \text{ } ^\circ\text{C}$ for 72 hours,
22
23 compared to the room temperature sample, along with the presence of CuO peaks, indicate a
24
25 higher oxidation level (*i.e.*, likely a thicker oxide layer) of the Cu NWs. In contrast, Raman
26
27 spectra of RG-O/ Cu NW hybrid films show only low-intensity peaks at around 214 cm^{-1} and
28
29 644 cm^{-1} due to the surface Cu₂O layer formed during the film fabrication processes. The spectra
30
31 of the hybrid films (72 hours at room temperature or at $60 \text{ } ^\circ\text{C}$) are similar to that of the pure Cu
32
33 NW films directly after fabrication (see Supporting Information).
34
35
36
37
38
39
40

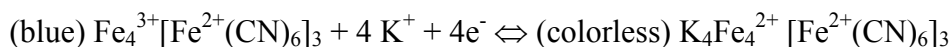
41 X-ray photoelectron spectroscopy (XPS) studies of these films (Figure 4c) at binding
42
43 energies of Cu 2p_{3/2} (932.4 eV) were done to further evaluate the possible protection against
44
45 oxidation by the RG-O film. The bottom spectrum in Figure 4c was obtained from pure Cu NW
46
47 films held at room temperature for 72 hours. The high intensity peak (dashed red curve) at
48
49 $\sim 932.4 \text{ eV}$ is assigned to the spectral overlap of Cu 2p_{3/2} and Cu₂O,²⁶ and the low intensity peak
50
51 (dotted blue curve) at $\sim 934.7 \text{ eV}$ is assigned to Cu(OH)₂.²⁷ The spectrum obtained from the Cu
52
53 NW film held at $60 \text{ } ^\circ\text{C}$ for 72 hours shows a peak that can be deconvoluted into peaks that
54
55
56
57
58
59
60

1
2
3 correspond to $\text{Cu}(\text{OH})_2$ (934.7 eV) (dotted blue curve), CuO (933.6 eV), and the shake-up
4
5 satellites of CuO (940.3 eV and 943.1 eV) (solid dark green curves).^{26, 28} The presence of
6
7 different copper oxides in the latter spectrum indicates the higher level of oxidation of the Cu
8
9 NW film held at 60 °C for 72 hours. These copper oxide compounds were not observed in the
10
11 XPS spectra of RG-O/Cu NW films, which are similar to that of the as-prepared Cu NW films
12
13 (see Supporting Information). These data show the high stability of the RG-O/Cu NWs films
14
15 against oxidation, and that the RG-O layer protects the underlying Cu NWs from oxidation.
16
17
18

19
20 Recent reports show the improved electrical conductivity of hybrid films composed of Cu
21
22 metal grids²⁹ and Cu NWs³⁰ assembled with graphene grown by chemical vapor deposition
23
24 (CVD). In contrast, our results on RG-O/Cu NW hybrid films provide a solution-based route to
25
26 fabricate both the single component and hybrid films. Additionally, compared to RG-O/Ag NW
27
28 hybrid films, reported in our previous work,¹⁸ RG-O/Cu NW films are more cost-effective as Cu
29
30 NWs that are significantly less expensive than Ag NWs.⁶ In addition, our results on oxidation-
31
32 resistance of RG-O/Cu NW hybrid films are consistent with the recent studies on the protection
33
34 of metal surfaces from oxidation with RG-O films¹⁷ and CVD-graphene grown onto metal
35
36 substrates.²⁴ Another approach to improve the oxidation resistance of Cu NW films is by coating
37
38 Cu NWs with a Ni shell that yields oxidation-resistant cupronickel NWs.¹⁰ However, compared
39
40 to RG-O, the Ni coating addresses only the oxidation of Cu NWs and lowers the aspect ratio of
41
42 the Cu NWs, which can adversely affect the optical transmittance of the films.³¹
43
44
45
46
47

48 The RG-O/Cu NW hybrid films were tested as a transparent electrode in Prussian blue
49
50 (PB) based electrochromic (EC) devices. Typical PB-based EC devices are composed of a PB
51
52 layer deposited onto an ITO transparent electrode. Electrochemical reactions, induced by an
53
54 applied external electric field, cause reversible modulations in the optical properties of PB layers.
55
56
57
58
59
60

1
2
3 Color changes from blue to colorless upon reduction are caused by the conversion of a mixed-
4 valence (Fe^{2+} , Fe^{3+}) compound into a single-valence (Fe^{2+}) compound (and *vice versa* upon
5 oxidation) that can be described as:^{32, 33}
6
7
8
9



12
13
14
15
16
17 In our studies, ITO electrodes were replaced by RG-O/Cu NW electrodes on glass
18 substrates. EC PB layers on top of the RG-O/Cu NW transparent electrodes have been
19 electrochemically deposited using an aqueous solution of 0.05 M hydrochloric acid (HCl), 0.05
20 M potassium hexacyanoferrate (III) ($\text{K}_3[\text{Fe}(\text{CN})_6]$), and 0.05 M iron(III) chloride (FeCl_3) in a
21 1:2:2 ratio.^{34, 35} Applying an external field between the RG-O/Cu NW electrode and a Pt counter
22 electrode, both immersed into the solution, results in the homogeneous deposition of PB layers
23 onto the RG-O/Cu NW electrode (See Supporting Information).^{33, 34}
24
25
26
27
28
29
30
31
32
33

34 Optical property modulation of the deposited PB layers by the redox process has been
35 tested using 1M KCl aqueous solution as an electrolyte (Figure 5a). Electrochemical reduction of
36 PB induced by an external voltage (-0.6 V to the RG-O/Cu NW TCF) yields colorless EC layers.
37 Application of a reverse external field induces an oxidation process, which generates mixed
38 valence compounds and yields a blue color of the EC layers. The optical transmittance
39 corresponding to the bleached ($T_{550} = 79.2\%$) and colored ($T_{550} = 36.4\%$) states of the PB are
40 shown in Figure 5b. Typical coloration and bleaching times for 90% transmittance change are 75
41 s and 95 s, respectively. These values are close to that of an EC device using the same PB EC
42 film and same electrolyte, but with an ITO electrode.³²⁻³⁴
43
44
45
46
47
48
49
50
51
52
53
54
55
56
57
58
59
60

1
2
3
4
5
6
7
8
9
10
11
12
13
14
15
16
17
18
19
20
21
22
23
24
25
26
27
28
29
30
31
32
33
34
35
36
37
38
39
40
41
42
43
44
45
46
47
48
49
50
51
52
53
54
55
56
57
58
59
60

Such PB EC films with reversible coloration/bleaching properties cannot be obtained using pure Cu NW transparent electrodes; indeed, a mixed transparent electrode (a glass substrate with one-half covered by pure Cu NW film and the other by RG-O/Cu NW hybrid film, Figure 5c, as prepared film) was made that shows this. Homogeneous PB layers were deposited on top of the electrode (Figure 5c, colored state). In electrochemical bleaching processes, the PB layers on top of the RG-O/Cu NW film have been completely bleached, while no bleaching of the PB layer deposited on the pure Cu NW film was observed (Figure 5c, bleached state). This is because pure Cu NWs form copper hexacyanoferrate compounds during the deposition of PB layers.³⁶⁻³⁸ During the process of formation of these compounds the Cu NW network(s) have been destroyed, and consequently this electrode lost its high electrical conductivity. Also, Cu NWs films immersed into the electrolyte solution partially delaminate from the substrate, which also leads to the loss of NW network conductivity. In contrast, in RG-O/Cu NW films, the RG-O layer protects the Cu NWs from reacting with the harsh solution used for PB deposition, which allows for repeatable cycling and homogeneous optical modulation of the PB EC layer, and there was no delamination of the RG-O/Cu NW hybrid films when immersed in the KCl solution.

CONCLUSION

A film composed of RG-O platelets assembled onto a Cu NW film layer yields hybrid films with improved electrical conductivity, 2-D film continuity (no empty regions such as gaps between NWs), higher oxidation-resistance, and better adhesion to the substrate, than pure Cu NW films. EC device performance demonstrates that RG-O, acting as a protective layer for Cu NWs in harsh environments, makes these types of hybrid TCFs suitable for a wider range of applications than pure metal NW films.

METHODS

Fabrication of Cu NW films. Cu NWs with a concentration of 1mg/mL in aqueous solution containing 1% diethylhydroxylamine (DEHA) to prevent oxidation, and 1% polyvinylpyrrolidone (PVP) to prevent aggregation, were purchased from NanoForge. Cu NWs were separated from the solution by centrifugation (2000 rpm for 5 min). After removing the supernatant, the NW sediment was re-dispersed in isopropyl alcohol (IPA) mixed with 3.0 vol% hydrazine monohydrate ($\text{N}_2\text{H}_4 \cdot \text{H}_2\text{O}$) to prevent oxidation of Cu NWs, by vortexing for 3-4 min. This process was repeated four times in order to remove the PVP from the NW suspension. A 1.2 mg/mL dispersion of Cu NWs in IPA (having well-dispersed Cu NWs, Figure 1) was used for spray-coating. Higher (> 1.2 mg/mL) concentrations of Cu NWs in the dispersion resulted in agglomerated NWs, and when spray coated these adversely affect Cu NW film optical properties. Repeated spray-coating yields the desired density of Cu NWs on the substrate. Between each sprayed pulse, complete drying of the sprayed droplets on the substrate was obtained. Keeping the substrate at about 60 °C and delicately blowing it with nitrogen gas accelerated the drying process.

Fabrication of RG-O films. Graphite oxide was produced from natural graphite (SP-1, Bay Carbon) using a modified Hummers method, as described elsewhere.³⁹ Aqueous dispersions of G-O at various concentrations were prepared by stirring graphite oxide solids in pure water (18.0 M Ω ·cm resistivity, purchased from Barnstead) for 3 hours, and then sonicating the resulting mixture (VWR B2500A-MT bath sonicator) for 45 minutes. The G-O dispersions were then spin-coated onto glass substrates using a spin speed of 4000 rpm for 2 min. The obtained G-O films were subsequently reduced using hydrazine monohydrate ($\text{N}_2\text{H}_4 \cdot \text{H}_2\text{O}$) vapour for 24

1
2
3 hours, keeping the samples at 90 °C.,¹⁸ and were then thermally annealed at 400 °C for one hour
4
5 in an Ar (95%) +H (5 %) gas mixture at 1 atm pressure. RG-O films, obtained by spin coating of
6
7 an aqueous G-O dispersion with a concentration of 1.0 mg/mL, possess $R_s = 36.6 \pm 4.7$ k Ω /sq,
8
9 $T_{550} = 95.5$ % and an average thickness of about 0.8 nm. The latter films were used to fabricate
10
11 RG-O/Cu NW hybrid films.
12
13

14
15 **Characterization of films.** SEM (Hitachi S-5500 SEM equipped with STEM), and
16
17 AFM (Park Systems Model XE-100 AFM) were used to characterize the structural properties of
18
19 the nanostructures and thin films. Optical transmittances (T) were measured using ultraviolet-
20
21 visible-near infrared (UV-VIS NIR) spectroscopy (Cary 5000) and spectroscopic ellipsometry
22
23 (J.A. Wollam M2000). R_s was measured with the four-probe van der Pauw method: four gold
24
25 electrodes were deposited on the film in a square configuration with dimensions of $\sim 6 \times 6$ mm².
26
27 Raman spectroscopy (WITEC Alpha300, $\lambda = 488$ nm, 100 \times objective) measurements were
28
29 carried out to study the oxidation of Cu NWs. XPS experiments were performed on a Kratos
30
31 Photoelectron Spectroscopy system equipped with an Al K_α monochromator X-ray source
32
33 operating at a power of 350 W. Binding energies were determined relative to the metallic copper
34
35 Cu 2p_{3/2} binding energy of 932.4 eV. Deconvolution of XPS spectra were obtained resolved by
36
37 fitting each peak with a combined Guassian-Lorentzian function after background subtraction.
38
39
40
41
42
43
44

45
46 *Acknowledgement.* This work was supported by a Tokyo Electron Ltd. (TEL)-customized
47
48 Semiconductor Research Corporation award (Project #2009-OJ-1873_development of graphene-
49
50 based transparent conductive films for display applications). We thank D. Toma, J. Li and J.
51
52 Faguet for discussion and comments. A. J. G. and S.H. D. gratefully acknowledge the CNPq,
53
54
55
56
57
58
59
60

1
2
3 INCT of Carbon Nanomaterials (CNPq), NENNAM (Pronex F. Araucária/CNPq), and CAPES
4
5 and CNPq for the scholarship.
6
7
8
9
10

11
12 *Supporting Information Available:* Synthesis and characterization of RG-O/Cu NW hybrid films;
13 additional information on Raman spectra and XPS data; and some details of electrochromic
14 devices are presented. This material is available free of charge *via* the Internet at
15
16
17
18
19
20 <http://pubs.acs.org>.
21
22
23
24
25
26

27 REFERENCES AND NOTES

28
29
30
31

- 32 1. Lyons, P. E.; De, S.; Elias, J.; Schamel, M.; Philippe, L.; Bellew, A. T.; Boland, J. J.;
33 Coleman, J. N. High-Performance Transparent Conductors from Networks of Gold
34 Nanowires. *J. Phys. Chem. Lett.*, **2011**, *2*, 3058 - 3062.
35
36
- 37 2. Azulai, D.; Belenkova, T.; Gilon, H.; Barkay, Z.; Markovich, G. Transparent Metal
38 Nanowire Thin Films Prepared in Mesostructured Templates. *Nano Lett.* **2009**, *9*, 4246 -
39 4249.
40
41
42
43
44
- 45 3. Leem, D. S.; Edwards, A.; Faist, M.; Nelson, J.; Bradley, D. D. C.; de Mello, J. C.
46 Efficient Organic Solar Cells with Solution-Processed Silver Nanowire Electrodes. *Adv.*
47 *Mater.* **2011**, *23*, 4371 - 4375.
48
49
50
51
52
- 53 4. Lee, J. Y.; Connor, S.T.; Cui, Y.; Peumans, P. Solution-Processed Metal Nanowire Mesh
54 Transparent Electrodes. *Nano Lett.* **2008**, *8*, 689 - 692.
55
56
57
58
59
60

- 1
2
3
4
5
6
7
8
9
10
11
12
13
14
15
16
17
18
19
20
21
22
23
24
25
26
27
28
29
30
31
32
33
34
35
36
37
38
39
40
41
42
43
44
45
46
47
48
49
50
51
52
53
54
55
56
57
58
59
60
5. Wu, H.; Hu, L.; Rowell, M. W.; Kong, D.; Cha, J. J.; McDonough, J. R.; Zhu, J.; Yang, Y.; McGehee, M. D.; Cui, Y. Electrospun Metal Nanofiber Webs as High-Performance Transparent Electrode. *Nano Lett.* **2010**, *10*, 4242 - 4248.
6. Rathmell, A. R.; Wiley, B. J. The Synthesis and Coating of Long, Thin Copper Nanowires to Make Flexible, Transparent Conducting Films on Plastic Substrates. *Adv. Mater.*, **2011**, *23*, 4798 - 4803.
7. Zhang, D.; Wang, R.; Wen, M.; Weng, D.; Cui, X.; Sun, J.; Li, H.; Lu, Y. Synthesis of Ultralong Copper Nanowires for High-Performance Transparent Electrodes. *J. Am. Chem. Soc.*, **2012**, *134*, 14283 - 14286.
8. Hu, L.; Kim, H. S.; Lee, J. Y.; Peumans, P.; Cui, Y. Scalable Coating and Properties of Transparent, Flexible, Silver Nanowire Electrodes. *ACS Nano* **2010**, *4*, 2955 - 2963.
9. Morgenstern, F. S. F.; Kabra, D.; Massip, S.; Brenner, T. J. K.; Lyons, P. E.; Coleman, J. N.; Friend, R. H. Ag-Nanowire Films Coated with ZnO Nanoparticles as a Transparent Electrode for Solar Cells, *Appl. Phys. Lett.* **2011**, *99*, 183307.
10. Rathmell, A. R.; Nguyen, M.; Miaofang Chi, M.; Wiley, B. J. Synthesis of Oxidation-Resistant Cupronickel Nanowires for Transparent Conducting Nanowire Networks. *Nano Lett.*, **2012**, *12*, 3193 - 3199.
11. Zhu, R.; Chung, C.-H.; Cha, K. C.; Yang, W.; Zheng, Y. B.; Zhou, H.; Song, T.-B.; Chen, C.-C.; Weiss, P. S.; Li, G.; *et al.* Fused Silver Nanowires with Metal Oxide Nanoparticles and Organic Polymers for Highly Transparent Conductors. *ACS Nano* **2011**, *5*, 9877 - 9882.
12. Gaynor, W.; Burkhard, G. F.; McGehee, M. D.; Peumans, P. Smooth Nanowire/Polymer Composite Transparent Electrodes. *Adv. Mater.* **2011**, *23*, 2905 - 2910.

- 1
2
3
4
5
6
7
8
9
10
11
12
13
14
15
16
17
18
19
20
21
22
23
24
25
26
27
28
29
30
31
32
33
34
35
36
37
38
39
40
41
42
43
44
45
46
47
48
49
50
51
52
53
54
55
56
57
58
59
60
13. Park, S.; Ruoff, R.S. Chemical Methods for the Production of Graphenes. *Nature Nanotech.* **2009**, *4*, 217 - 224.
14. Wu, J. B.; Agrawal, M.; Becerril, H. A.; Bao, Z. N.; Liu, Z. F.; Chen, Y. S.; Peumans, P. Organic Light-Emitting Diodes on Solution-Processed Graphene Transparent Electrodes. *ACS Nano* **2010**, *4*, 43 - 48.
15. Becerril, H. A.; Mao, J.; Liu, Z.; Stoltenberg, R. M.; Bao, Z.; Chen, Y. Evaluation of Solution-Processed Reduced Graphene Oxide Films as Transparent Conductors. *ACS Nano* **2008**, *2*, 463 - 470.
16. Eda, G.; Chhowalla, M.; Chemically Derived Graphene Oxide: Towards Large-Area Thin-Film Electronics and Optoelectronics. *Adv. Mater.* **2010**, *22*, 2392 - 2415.
17. Kang, D.; Kwon, J. Y.; Cho, H.; Sim, J.-H.; Hwang, H. S.; Kim, C. S.; Kim, Y. J.; Ruoff, R. S.; Shin, H. S. Oxidation Resistance of Iron and Copper Foils Coated with Reduced Graphene Oxide Multilayers. *ACS Nano* **2012**, *6*, 7763 - 7769.
18. Kholmanov, I. N.; Stoller, M.; Edgeworth, J.; Lee, W. H.; Li, H.; Lee, J.; Barnhart, C.; Potts, J.; Piner, R.; Akinwande, D.; *et al.* Nanostructured Hybrid Transparent Conductive Films with Antibacterial Properties. *ACS Nano* **2012**, *6*, 5157 - 5163.
19. Yamaguchi, H.; Eda, G.; Mattevi, C.; Kim, H. K.; Chhowalla, M. Highly Uniform 300 mm Wafer-Scale Deposition of Single and Multilayered Chemically Derived Graphene Thin Films. *ACS Nano* **2010**, *4*, 524 - 528.
20. Suk, J. W.; Kitt, A.; Magnuson, C. W.; Hao, Y.; Ahmed, S.; An, J.; Swan, A. K.; Goldberg, B. B.; Ruoff, R. S. Transfer of CVD-Grown Monolayer Graphene onto Arbitrary Substrates. *ACS Nano* **2011**, *5*, 6916 - 6924.

- 1
2
3
4
5
6
7
8
9
10
11
12
13
14
15
16
17
18
19
20
21
22
23
24
25
26
27
28
29
30
31
32
33
34
35
36
37
38
39
40
41
42
43
44
45
46
47
48
49
50
51
52
53
54
55
56
57
58
59
60
21. Kholmanov, I. N.; Magnuson, C. W.; Aliev, A. E.; Li, H.; Zhang, B.; Suk, J. W.; Zhang, L. L.; Peng, E.; Mousavi, S. H.; Khanikaev, A. B.; *et al.* Improved Electrical Conductivity of Graphene Films Integrated with Metal Nanowires. *Nano Lett.* **2012**, *12*, 5679 - 5683.
22. Yen, M.-Y.; Hsiao, M.-C.; Liao, S.-H.; Liu, P.-I.; Tsai, H.-M.; Ma, C.-C. M.; Pu, N.-W.; Ger, M.-D. Preparation of Graphene/Multi-Walled Carbon Nanotubes Hybrid and Its Use as Photoanodes of Dye-Sensitized Solar Cells. *Carbon*, **2011**, *49*, 3597 - 3606.
23. Chou, M. H.; Liu, S. B.; Huang, C. Y.; Wu, S. Y.; Cheng, C. L. Confocal Raman Spectroscopic Mapping Studies on a Single CuO Nanowire. *Appl. Surf. Sci.* **2008**, *254*, 7539 - 7543.
24. Chen, S.; Brown, L.; Levendorf, M.; Cai, W.; Ju, S. -Y.; Edgeworth, J.; Li, X.; Magnuson, C. W.; Velamakanni, A.; Piner, R. D.; *et al.* Oxidation Resistance of Graphene-Coated Cu and Cu/Ni Alloy. *ACS Nano*, **2011**, *5*, 1321 - 1327.
25. Niaura, G. Surface-Enhanced Raman Spectroscopic Observation of Two Kinds of Adsorbed OH-Ions at Copper Electrode. *Electrochim. Acta* **2000**, *45*, 3507 - 3519.
26. Wu, C.-K.; Yin, M.; O'Brien, S.; Koberstein, J. T. Quantitative Analysis of Copper Oxide Nanoparticle Composition and Structure by X-ray Photoelectron Spectroscopy. *Chem. Mater.* **2006**, *18*, 6054 - 6058.
27. Dubè, E. C.; Workie, B.; Kounaves, S. P.; Robbat, A., Jr.; Aksu M. L.; Davies, G. Electrodeposition of Metal Alloy and Mixed Oxide Films Using a Single-Precursor Tetranuclear Copper-Nickel Complex. *J. Electrochem. Soc.* **1995**, *142*, 3357 - 3365.
28. Poulston, S.; Parlett, P. M.; Stone, P.; Bowker, M. Surface Oxidation and Reduction of CuO and Cu₂O Studied Using XPS and XAES. *Surf. Interface Anal.* **1996**, *24*, 311 - 320.

- 1
2
3
4
5
6
7
8
9
10
11
12
13
14
15
16
17
18
19
20
21
22
23
24
25
26
27
28
29
30
31
32
33
34
35
36
37
38
39
40
41
42
43
44
45
46
47
48
49
50
51
52
53
54
55
56
57
58
59
60
29. Zhu, Y.; Sun, Z.; Yan, Z.; Jin, Z.; Tour, J. M. Rational Design of Hybrid Graphene Films for High-Performance Transparent Electrodes. *ACS Nano* **2011**, *5*, 6472–6479.
30. Liang, J.; Bi, H.; Wan, D.; Huang, F. Novel Cu Nanowires/Graphene as the Back Contact for CdTe Solar Cells. *Adv. Func. Mater.* **2012**, *22*, 1267 – 1271.
31. Sorel, S.; Lyons, P. E.; De, S.; Dickerson, J. C.; Coleman, J. N. The Dependence of the Optoelectrical Properties of Silver Nanowire Networks on Nanowire Length and Diameter, *Nanotechnology*, **2012**, *23*, 185201.
32. Lundgren, C. A.; Murray, R. W. Observations on the Composition of Prussian Blue Films and Their Electrochemistry. *Inorg. Chem.* **1988**, *27*, 933 - 939.
33. Karyakin, A. A. Prussian Blue and Its Analogues: Electrochemistry and Analytical Applications. *Electroanal.* **2001**, *13*, 813 - 819.
34. Lupu, S.; Mihailciuc, C.; Pigani, L.; Seeber, R.; Totir, N.; Zanardi, C. Electrochemical Preparation and Characterisation of Bilayer Films Composed by Prussian Blue and Conducting Polymer. *Electrochem. Commun.* **2002**, *4*, 753 - 758.
35. Nossol, E.; Zarbin, A. J. G., Electrochromic Properties of Carbon Nanotubes/Prussian Blue Nanocomposite Films. *Sol. Energ. Mat. Sol. C.* **2013**, *109*, 40 - 46.
36. Chen, S. M.; Chan, C. M. Preparation, Characterization, and Electrocatalytic Properties of Copper Hexacyanoferrate Film and Bilayer Film Modified Electrodes. *J. Electroanal. Chem.* **2003**, *543*, 161 - 173.
37. Makowski, O.; Stroka, J.; Kulesza, P. J.; Malik, M. A.; Zbigniew, G. Electrochemical Identity of Copper Hexacyanoferrate in the Solid-State: Evidence for the Presence and Redox Activity of Both Iron and Copper Ionic Sites. *J. Electroanal. Chem.* **2002**, *532*, 157 - 164.

1
2
3 38. F. Adekola, F.; Fedoroff, M.; Ayrault, S.; Loos-Neskovic, C.; Garnier, E.; Yu, L. T.

4
5 Interaction of Silver Ions in Solution with Copper Hexacyanoferrate (II) $\text{Cu}_2\text{Fe}(\text{CN})_6$. *J.*

6
7
8 *Solid State Chem.* **1997**, *132*, 399 - 406.

9
10 39. Stankovich, S.; Dikin, D. A.; Dommett, G. H. B.; Kohlhaas, K. M.; Zimney, E. J.; Stach,

11
12 E. A.; Piner, R. D.; Nguyen, S.B. T.; Ruoff, R. S. Graphene-Based Composite Materials.

13
14
15 *Nature* **2006**, *442*, 282 - 286.
16
17
18
19
20
21
22
23
24
25
26
27
28
29
30
31
32
33
34
35
36
37
38
39
40
41
42
43
44
45
46
47
48
49
50
51
52
53
54
55
56
57
58
59
60

Figure captions.

Figure 1. a) SEM image of a network of Cu NWs on a SiO₂/Si substrate. b) AFM image of RG-O films on a SiO₂/Si substrate. The line profile shows a smooth surface. c) Optical transmittance and sheet resistance of spin coated RG-O and spray coated Cu NW films.

Figure 2. a) Schematic of preparation of RG-O/Cu NW hybrid films. b) Photographs of G-O dispersed in water (1.0 mg/mL) and Cu NWs dispersed in IPA with 3.0 vol% N₂H₄ · H₂O (1.2 mg/mL). c) RG-O (top) and Cu NW (bottom) films on glass substrates. d) 2 × 2 cm² PMMA/RG-O film delaminated from the glass substrate in 1M aqueous solution of NaOH. e) Photograph of 2 × 2 cm² RG-O/Cu NW films on a glass substrate after the PMMA layer was removed.

Figure 3. a) Transmittance and sheet resistance of the pure Cu NW films and RG-O/Cu NW hybrid films. b) SEM image of individual RG-O platelets with lateral sizes indicated. c) SEM image of a typical RG-O/Cu NW film.

Figure 4. a) Changes in R_s of pure Cu NW films and RG-O/Cu NW hybrid films kept at room temperatures (RT) and also at 60 °C, each for 72 hours. b) Raman spectra of Cu NW films kept at room temperature (bottom) and 60°C (middle) 72 hours, and of RG-O/Cu NW films kept at 60 °C for 72 hours (top). c) Cu 2p_{3/2} XPS spectrum of Cu NW film kept at room temperature (bottom), and 60 °C (middle) for 72 hours, and of RG-O/Cu NW films kept at 60 °C for 72 hours (top).

1
2
3 **Figure 5.** a) Schematic of an electrochromic device in an electrolyte solution. b) Optical
4 transmittance spectra of colored and bleached states of PB films deposited on a RG-O/Cu NW
5 transparent electrode. c) As-prepared mixed transparent electrode composed of pure Cu NW
6 films (left) and RG-O/Cu NW films (right). Initial (colored) state (right top) and bleached state
7
8
9
10
11
12
13 (right bottom) of PB deposited on the mixed electrode.
14
15
16
17
18
19
20
21
22
23
24
25
26
27
28
29
30
31
32
33
34
35
36
37
38
39
40
41
42
43
44
45
46
47
48
49
50
51
52
53
54
55
56
57
58
59
60

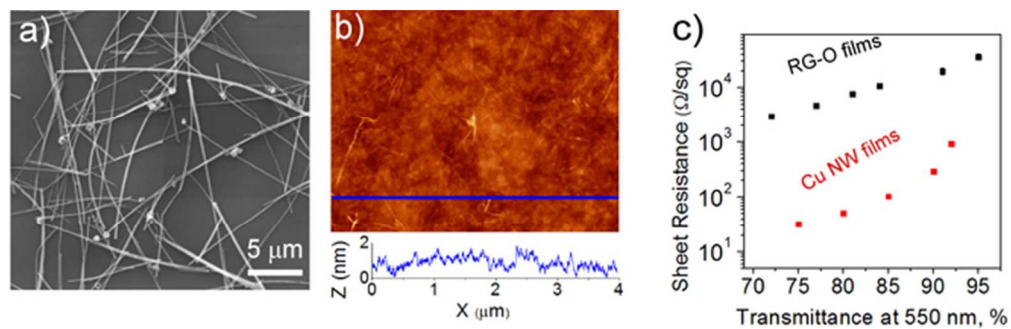


Figure 1. a) SEM image of a network of Cu NWs on a SiO₂/Si substrate. b) AFM image of RG-O films on a SiO₂/Si substrate. The line profile shows a smooth surface. c) Optical transmittance and sheet resistance of spin coated RG-O and spray coated Cu NW films.
55x17mm (300 x 300 DPI)

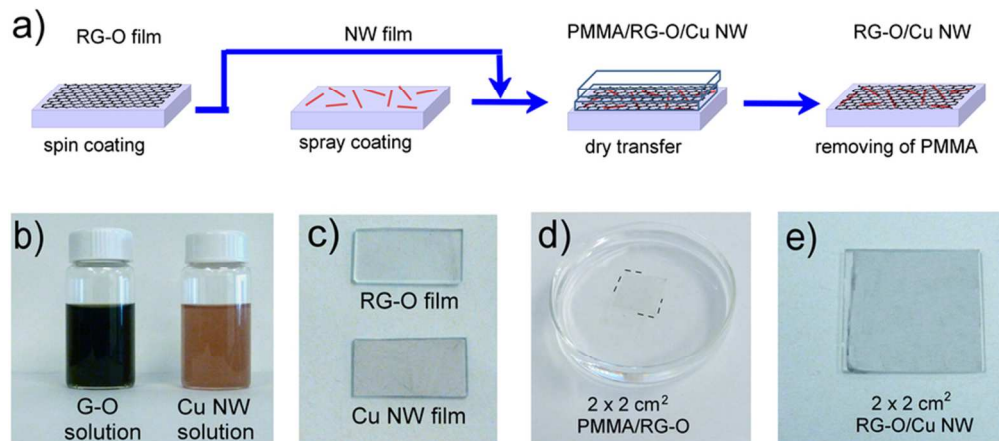


Figure 2. a) Schematic of preparation of RG-O/Cu NW hybrid films. b) Photographs of G-O dispersed in water (1.0 mg/mL) and Cu NWs dispersed in IPA with 3.0 vol% $\text{N}_2\text{H}_4 \cdot \text{H}_2\text{O}$ (1.2 mg/mL). c) RG-O (top) and Cu NW (bottom) films on glass substrates. d) $2 \times 2 \text{ cm}^2$ PMMA/RG-O film delaminated from the glass substrate in 1M aqueous solution of NaOH. e) Photograph of $2 \times 2 \text{ cm}^2$ RG-O/Cu NW films on a glass substrate after the PMMA layer was removed.

78x34mm (300 x 300 DPI)

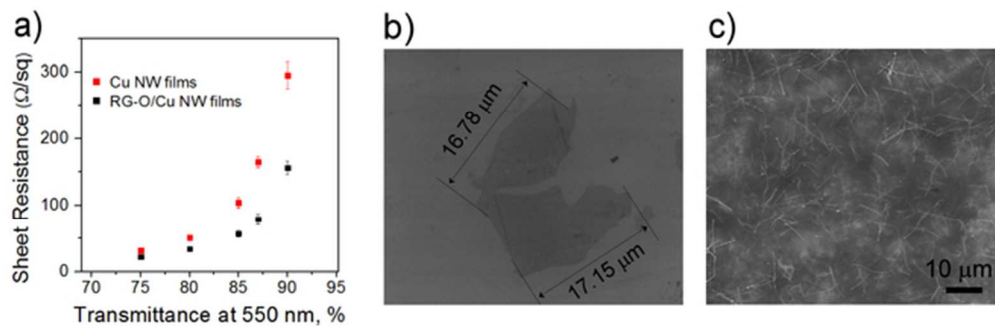


Figure 3. a) Transmittance and sheet resistance of the pure Cu NW films and RG-O/Cu NW hybrid films. b) SEM image of individual RG-O platelets with lateral sizes indicated. c) SEM image of a typical RG-O/Cu NW film.

55x17mm (300 x 300 DPI)

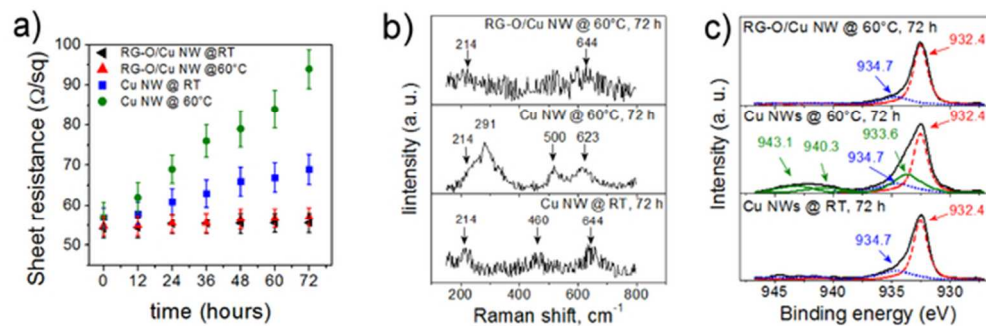


Figure 4. a) Changes in R_s of pure Cu NW films and RG-O/Cu NW hybrid films kept at room temperatures (RT) and also at 60 °C, each for 72 hours. b) Raman spectra of Cu NW films kept at room temperature (bottom) and 60°C (middle) 72 hours, and of RG-O/Cu NW films kept at 60 °C for 72 hours (top). c) Cu 2p_{3/2} XPS spectrum of Cu NW film kept at room temperature (bottom), and 60 °C (middle) for 72 hours, and of RG-O/Cu NW films kept at 60 °C for 72 hours (top).

55x17mm (300 x 300 DPI)

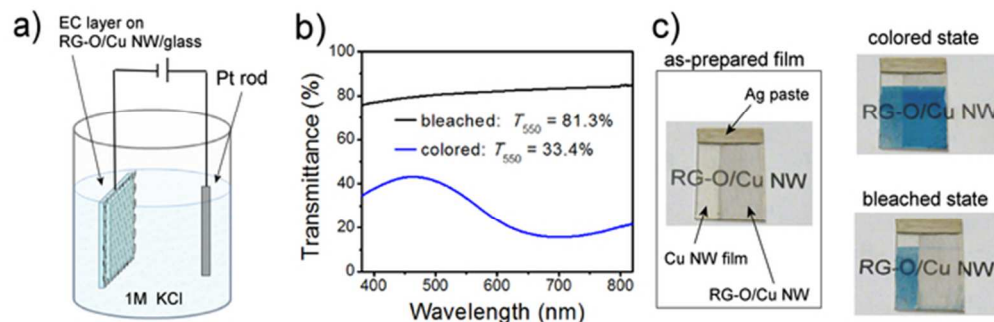
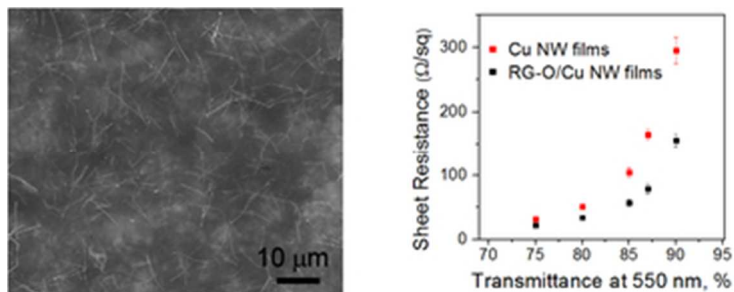


Figure 5. a) Schematic of an electrochromic device in an electrolyte solution. b) Optical transmittance spectra of colored and bleached states of PB films deposited on a RG-O/Cu NW transparent electrode. c) As-prepared mixed transparent electrode composed of pure Cu NW films (left) and RG-O/Cu NW films (right). Initial (colored) state (right top) and bleached state (right bottom) of PB deposited on the mixed electrode. 55x17mm (300 x 300 DPI)



Abstract. Hybrid films composed of reduced graphene oxide (RG-O) and Cu nanowires (NWs) were prepared. Compared to Cu NW films, the RG-O/Cu NW hybrid films have improved electrical conductivity, oxidation-resistance, substrate adhesion, and stability in harsh environments. The RG-O/Cu NW films were used as transparent electrodes in Prussian blue (PB)-based electrochromic devices where they performed significantly better than pure Cu NW films.

31x12mm (300 x 300 DPI)